Supplementary Materials for

Dopaminylation of histone H3 in ventral tegmental area regulates cocaine seeking

Ashley E. Lepack, Craig T. Werner, Andrew F. Stewart, Sasha L. Fulton, Ping Zhong, Lorna A. Farrelly, Alexander C. W. Smith, Aarthi Ramakrishnan, Yang Lyu, Ryan M. Bastle, Jennifer A. Martin, Swarup Mitra, Richard M. O'Connor, Zi-Jun Wang, Henrik Molina, Gustavo Turecki, Li Shen, Zhen Yan, Erin S. Calipari, David M. Dietz, Paul J. Kenny, Ian Maze*

*Corresponding author. Email: ian.maze@mssm.edu

Published 10 April 2020, *Science* **368**, 197 (2020)
DOI: 10.1126/science.aaw8806

This PDF file includes:

Other Supplementary Material for this manuscript includes the following:
(available at science.sciencemag.org/content/368/6487/197/suppl/DC1)

Tables S1 to S5 (.xlsx)

Materials and Methods

Human Postmortem Brain Tissues

Post-mortem human VTA tissues were obtained from the Douglas – Bell Brain Bank (IRB approval for tissue banking – Douglas Mental Health University Institute, Montreal, Quebec, Canada). Tissue preservation was achieved as previously described (*16*). Brains were placed on wet ice and transported to the Douglas – Bell Brain Bank facilities. Tissues were flash frozen in 2-methylbutane at −40 °C, dissected and stored in sections conserving anatomical landmarks at −80 °C. VTA tissues were later sectioned from frozen slices.

All subjects died suddenly without prolonged medical illness or extended agonal states. For each case, the cause of death was determined by the Quebec Coroner Office, and toxicological screens were performed to obtain information on medication and illicit substance use at their time of death. The subject group consisted of 11 individuals (all male Caucasian) who met the Structured Clinical Interview for DSM-IV (Diagnostic and Statistical Manual of Mental Disorders-IV) Axis I Disorders: Clinician Version (SCID-I) criteria for cocaine dependence. The control group comprised 8 subjects (six male and two female Caucasians) with no history of cocaine dependence. Groups were matched for subject age, post-mortem interval and pH. For all subjects, psychological autopsies were performed giving us access to detailed information on psychiatric and medical histories, as well as other relevant clinical and sociodemographic data.

Animals

Male Sprague-Dawley rats (Charles River Laboratories; 300-375 g or Envigo; 250-300 g) were pair housed and maintained on a 12 h reverse light/dark cycle with food and water available *ad libitum*. $Tgm2^{fl/fl}$ mice were purchased from The Jackson Laboratory (Stock #024694) and were bred on a C57BL/6J background. All procedures were done in accordance with NIH guidelines and the Institutional Animal Care and Use Committees of the Icahn School of Medicine at Mount Sinai and the State University of New York at Buffalo.

Jugular Catheterization

Catheters were comprised of 14 cm long silastic tubing (inner tubing; 0.012 x 0.025 in., Dow Corning, Midland, MI, USA) connected to a bent metal cannula (22 gauge) covered by 1.5 cm of silastic tubing (outer tubing; 0.025 x 0.047 in., Dow Corning, Midland, MI, USA), with a small ball of silicone 3 cm before the bottom of the inner tubing. Briefly, animals were anaesthetized by inhalation of ~3% isoflurane in oxygen throughout the entire surgical period. Incisions were made in clean-shaven areas on the mid-back, as well as on the chest above the jugular vein. Catheters were passed subcutaneously and mounted on the rats' backs. A small incision was made in the jugular vein and catheters were inserted until they were flush with the silicone ball and secure to the vein (*17*). Both back and chest incisions were sutured and then treated with topical antibiotics and an anti-inflammatory analgesic (meloxicam; 1 mg/kg, s.c.) for 3 days post-surgery. Animals were flushed daily with heparin + Baytril (1mg/ml; 0.1 mg/ml) to maintain catheter patency and to reduce bacterial infections. Animals were singly housed following surgery.

Cocaine Self-Administration (SA)

Prior to jugular catheterization, animals were food restricted (20 g per day; 3-4 days) and trained to respond to the 'active' lever on a fixed ratio (FR) schedule 1 of reinforcement for food pellets (1 hr sessions per day). Following successful learning (~100 pellets per session), animals were implanted with jugular catheters and then given 5 days to recover before cocaine SA. Catheter patency was tested with 1 mg methohexital sodium (Brevital; Sigma-Aldrich, St. Louis, MO) the day prior to cocaine SA. Animals were then trained to respond on an 'active' lever for cocaine hydrochloride diluted in 0.9% sterile saline, 1mg/kg/infusion IV (0.1 ml injection volume delivered over 4 s), with a 20 s timeout in between each infusion, which was indicated by a cue light located directly above the 'active' lever; responding on the lever was recorded but without consequence. Rodents were trained on this paradigm at a FR 1 (2 days), FR3 (1 day) and then FR5 (2 days; 1 hr sessions). Following completion of successful learning at FR5 (~15 rewards total), rodents were equally divided into restricted access (1 hr session) or extended access (6 hr sessions) groups for 10 days, with each cocaine infusion resulting in delivery of 0.5mg/kg/infusion of cocaine. Additionally, a separate group of rodents were put through the same paradigm but were only allowed to respond for saline (0.9%) (non-reinforcement controls). For molecular analyses, cocaine *vs.* saline animals were euthanized immediately, 24 hr or 30 days after the last infusion.

For yoked experiments, animals were catheterized and then matched to individual rats in the extended access groups to receive the same amount and frequency of infusions. For food SA, animals were trained similarly to that of cocaine rats to respond to an 'active' lever at a FR5 for food pellets before being switched to an extended access paradigm.

Rats in the food SA group were kept at ~80% body weight throughout the experiment. To investigate molecular changes following experimenter-administered (EA) cocaine, rats were given 10 days of cocaine (10 mg/kg) via intraperitoneal (i.p.) injections. For all molecular analyses using these groups, rats were euthanized 30 days post the last infusion/reward/injection.

Preparation of Dopaminylated Peptides for Antibody Generation & Dot Blots

Peptide immunogens corresponding to H3 (1-10, Q5dop or K4me3Q5dop) were prepared using standard Fmoc-strategy solid phase chemistry on a 2-Cl Trityl resin incorporating a C-terminal Cys residue for conjugation to maleimide-activated KLH. Orthogonally protected Fmoc-Glu(OAll)-OH was incorporated at position 5 for on-resin dopaminylation, and Fmoc-Lys(me3)-OH was coupled at position 4 to generate the dual modified immunogen. Following assembly of the peptide backbones, resin-bound peptides were allyl deprotected by treatment with $Pd(0)(PPh_3)_4$ (0.2 equiv.), N,N-dimethylbarbituric acid (10 equiv.) in DCM for 30 min (two treatments). The resins were then washed extensively with DCM and DMF to remove residual Pd. The Glu5 sidechain carboxylate was dopaminylated by two treatments with PyAOP (1.1 equiv.) and DIEA (4.0 equiv.) in DMF, followed by direct addition of dopamine acetonide (2.0 equiv.) and agitation for 30 min. Dopamine acetonide was prepared in an identical fashion as previously reported (*18*) in three steps from dopamine hydrochloride involving N-trifluoroacetamide protection, acetonide formation and N-trifluoroacetamide deprotection. The crude dopaminylated peptides were cleaved from the resin with concomitant global deprotection (including acetonide removal) via treatment with 5% ethanedithiol (EDT), 2.5% iPr_3SiH, 2.5% H_2O in TFA for 2 hr at RT. Peptides were

purified by preparative C-18 RP-HPLC, and final products were characterized by analytical C-18 RP-HPLC and ESI-MS. The purified peptides were then provided to EMD Millipore for generation of rabbit polyclonal antibodies, as described below. Similar procedures were also employed to generate H3 (1-15) dopaminylated peptides for dot blot analyses.

Western Blotting and Antibodies

VTA tissues were collected from rats (2 mm punches) and immediately frozen. To purify nuclear fractions from VTA, punches were homogenized in Buffer A containing 10 mM HEPES (pH 7.9), 10 mM KCl, 1.5 mM $MgCl_2$, 0.34 M sucrose, 10% glycerol, 1 mM EDTA, 1X protease inhibitor cocktail and 1X phosphostop inhibitor. Following homogenization, 0.1% TritonX-100 was added to each homogenate, incubated on ice for 30 min and then centrifuged for 5 min at 1300g at 4° C. Supernatants containing cytosolic fractions were discarded, and nuclear pellets were resuspended in Buffer A to remove any remaining cytosolic contamination, followed by centrifugation for 5 min at 1300g at 4° C. After centrifugation, supernatants were discarded and pellets were resuspended and sonicated in sample buffer containing 0.3 M sucrose, 5 mM HEPES, 1% SDS and 1X protease inhibitor cocktail. Protein concentrations were measured using the DC protein assay kit (BioRad), and 10-15 ug of protein was loaded onto 4-12% NuPage BisTris gels (Invitrogen) for electrophoresis. Proteins were then transferred to nitrocellulose membranes and blocked for 1 hr in 5% milk in PBS + 0.1% Tween 20 (PBST), followed by incubation with primary antibodies overnight at 4° C, with the exception of anti-H3Q5dop, which was incubated for two days at 4° C. For competition assays, antibodies were pre-incubated with indicated peptides at a 5:1 ratio for 1 hr at RT

before being incubated with the membrane. The following antibodies were used: rabbit anti-H3Q5dop (1:200, ABE2588; MilliporeSigma), rabbit anti-H3K4me3Q5dop (1:500, ABE2590; MilliporeSigma), rabbit anti-H3K4me3 (1:1000, lot #: GR273043-6, Abcam ab8580), mouse anti-Tgm2 (1:500, lot #: Gr3188112-4, Abcam ab2386), rabbit anti-Tgm2 (1:500, lot #: 3, Cell Signaling D11A6), rabbit anti-H3Q5ser (1:500, ABE1791; MilliporeSigma) and rabbit anti-H3 (1:50000, lot #: GR293151-1, Abcam ab1791). The next day, membranes were washed 3X in PBST (10 min) and incubated for 1 hr with horseradish peroxidase conjugated anti-rabbit (BioRad 170-6515, lot #: 64033820) or anti-mouse (GE Healthcare UK Limited NA931V, lot #: 9814763) secondary antibodies (1:10000; 1:50000 for anti-H3 antibody, BioRad) in 5% milk/PBST at RT. After three final washes with PBST, bands were detected using enhanced chemiluminescence (ECL; Millipore). Densitometry was used to quantify protein bands using Image J Software (NIH), and proteins were normalized to total H3. Direct blue staining was sometimes used as a loading control.

For peptide dot blots, peptides were dotted as progressive protein concentrations (0.25, 0.5, 1, 2ug) on a nitrocellulose membrane. Membranes were left to dry at RT for 1 hr and then blocked in 5% milk/PBST for 1 hr. Membranes were treated similar to that described above.

Enzymatic Assays

For assessments of TGM2-mediated transamidation of dopamine or serotonin to recombinant H3.2 protein [as previously described in (*1*)], 0.25 ug guinea pig Tgm2 (Zedira, T006), 5 mM dopamine or serotonin (Sigma) and 10 ug of recombinant H3.2

were combined with enzymatic buffer containing 250 mM tris-acetate (pH 7.5), 8.75mM $CaCl_2$ and 1X protease inhibitor cocktail, followed by incubation for 3 hr at RT. Following incubation, enzymatic reactions were boiled with laemmli buffer and then run on 4-12% NuPage BisTris gels (Invitrogen). Nitrocellulose membranes were blocked in 5% milk/PBST for 1 hr and then incubated with primary antibody (anti-H3Q5dop or H3Q5ser) overnight. Enzymatic assays were also performed using serotonin and norepinephrine to confirm the specificity of our in-house anti-H3Q5dop antibody. Enzymatic assays were additionally performed using reconstituted unmodified *vs.* K4me3 mononucleosomes from Active Motif.

LC-MS/MS validation of dopaminylayted H3 (1-15)

Samples were analyzed by LC-MS/MS (Dionex 3000 coupled to Q-Exactive, Thermo Fisher). Peptides were separated by C-18 chromatography (inner diameter of 75 μm/3μm particles, Nikkyo Technologies, Japan) using a gradient increasing from 1% B to 35% B in 16 minutes (A: 0.1% formic acid, B: acetonitrile in 0.1% formic acid). The mass spectrometer was operated in PRM mode[11] (Resolution 35,000, AGC target, 5e5, max. inject time of 60ms and an isolation window of m/z of 2.0). MS was acquired from m/z 300-1650 while m/z = 100 was set as lowest mass for MS/MS. Charge states 2+ to 5+ of the modified and non-modified peptides were targeted. An energy of 25 NCE was used for the quadruply charged peptide: ARTKQTARKSTGGKA-NH_2, with and without modification. Supplemental fig. 1d represents a high resolution, high accuracy tandem mass spectra (sample +DA/+TGM2) of the quadruply charged peptide ARTKQTARKSTGGKA-NH2 modified by DA at Gln 5 (m/z 424.7466 [-0.42 ppm]). The full amino acid sequence was accounted for. Fragment ions (y and b) used to validate the dopaminylated glutamine are annotated in the tandem MS spectrum.

Lentiviral and AAV Constructs

Lentiviral constructs were generated as previously described (*1*). Briefly, lenti-H3.3 constructs [wildtype (WT) vs. (Q5A)-Flag-HA] were cloned into a pCDH-RFP vector (empty) by PCR and restriction digestion. Purified plasmids were sent to GENEWIZ for sequence validation. pCDH-RFP-H3.3 plasmids were then sent to Cyagen Biosciences for lentiviral packaging at high titer. Note that the H3.3 Q5A vector used in these studies, which does not affect adjacent H3K4me3, is predicted to inhibit the expression of all modifications on Q5. However, appreciable signal for additional monoaminyl marks (e.g., H3Q5ser) are not observed in VTA *vs.* H3Q5dop (fig. S3, E). Adeno-associated viral vector particles (AAV-GFP and AAV-Cre-GFP) were provided by Dr. Eric Nestler (ISMMS).

Viral Infusion

24 hr following the last day of cocaine *vs.* saline SA (day 11), animals were anaesthetized with a ketamine/xylazine solution (80/6 mg/kg) i.p., positioned in a stereotaxic frame (Kopf instruments) and 1 μl of viral construct was infused bilaterally into VTA using the following coordinates; anterior-posterior (AP) -4.9, medial-lateral (ML) +2.1, dorsal-ventral (DV) -7.6. Following surgery, rats received meloxicam (1 mg/kg) s.c. and topical antibiotic treatments for 3 days. All tissue collections or behavioral testing commenced 30 days after surgery to allow for both maximal expression of the viral constructs and a significant withdrawal period.

Immunohistochemistry

Rats were anaesthetized with ketamine/xylazine (80/6 mg/kg) i.p., and then perfused transcardially with cold phosphate buffered saline (PBS 1X) followed by 4% paraformaldehyde (PFA) in 1X PBS. Next, brains were post-fixed in 4% PFA overnight at 4° C and then transferred into 30% sucrose/PBS 1X for two days. Brains were then cut into serial 40 μm coronal slices. Free floating VTA slices were washed 3X in tris buffered saline (TBS 1X), incubated for 30 min in 0.2% Triton X/TBS 1X–to permablilize tissue–and then incubated for 1 hr at RT in blocking buffer (0.3% Triton X, 3% donkey serum, 1X TBS). Brain slices were then incubated overnight at RT with mouse anti-RFP (1:200; lot#: GR3181906-1, Abcam ab65856) and HA-488 (1:200; lot #: K1716, Life Technologies, Alexa Fluor SC-805). The next day, brain slices were washed 3X in 1X TBS and then incubated for 2 hr at RT with a fluorescent-tagged Alexa Fluor 568 anti-mouse secondary antibody (1:500, lot #: 1218263, Life Technologies A11004). Brain sections were then washed 3X in 1X TBS, incubated with DAPI (1:10000, lot #: RK2297251, Thermo Scientific 62248) for 5 min at RT, mounted on Superfrost Plus slides (Fischer Scientific) and then coverslipped with Prolong Gold (Invitrogen). Immunofluorescence was visualized using a confocal microscope (Zeiss LSM 780).

RNA-sequencing

Animals were exposed to extended access SA for 10 days and then injected bilaterally intra-VTA with lenti-empty, lenti-H3.3 WT or lenti-H3.3 Q5A the following day. Animals were then put through WD for 30 days, and then euthanized with their brains being flash frozen. Brains were sectioned at 150 μm on a cryostat, and RFP was illuminated using a NIGHTSEA BlueStar flashlight to microdissect virally infected tissues. VTA tissue punches were homogenized in Trizol (Thermo Fisher), and RNA was

isolated on RNeasy Microcolumns (Qiagen) following manufacturer's instructions. RNA concentrations were assessed using a nanodrop spectrophotometer and RNA 260/280 and 260/230 ratios were confirmed at >1.8. Following RNA purification, RNA-seq libraries were prepared according to Illumina protocols and sequenced on an Illumina HiSeq 4000 (or equivalent) sequencer.

Following sequencing, raw sequencing reads from rat VTA were mapped to rn6 using HISAT2v2.1.0. Counts of reads mapping to genes were obtained using featureCounts against Ensembl v90 annotation. Differential expression analysis was done using the DESeq2 package (v1.6.3) at a p-value cutoff of 0.05. RRHO maps were generated as previously described (*19*). Kegg 2019 (via Enrichr) was performed to assess pathway enrichment for differentially expressed genes (*20-22*).

Electrophysiology

For stereotaxic delivery of viruses, male Sprague Dawley rats (P20-21 upon arrival; Envigo) were injected with syringes set at a 10° angle [measurements on the surface of the skull from bregma taken in mm: AP: −4.9, ML: +2.2, DV: −7.6 (*23*)]. Viruses were manually infused at a rate of 0.2 μl/min for a total of 1.0 μl per hemisphere, and the injectors were left in place for an additional 10 min to allow for diffusion. When viruses were maximally expressed, rats were used for electrophysiology experiments, as described below.

Rats were anesthetized with isoflurane for ~30 sec and decapitated quickly. Coronal slices (300 μm) containing VTA were cut with a vibratome (Leica VT1000s) in ice-cold sucrose solution (in mM: 234 sucrose, 4 $MgSO_4$, 2.5 KCl, 1 NaH_2PO_4, 0.1 $CaCl_2$, 15

HEPES, 11 glucose, pH 7.35) and immediately incubated in artificial cerebrospinal fluid (ACSF) (in mM: 128 NaCl, 26 $NaHCO_3$, 3KCl, 5 $MgCl_2$, 1.25 NaH_2PO_4, 1 $CaCl_2$, 10 Glucose, pH 7.4, and 300 mOsm) oxygenated with 95% O_2+5%CO_2) for ~1 hour at 34 ^oC. Next, slices were transferred to a low Mg^{2+}, high Ca^{2+} recording ACSF (in mM: 2 $MgCl_2$, 2 $CaCl_2$) and incubated for 40 min at RT (22 ^oC) before recording.

During recording, infected VTA DA neurons were selected based on cell morphology (large soma size) (*24*). Their identity was confirmed by their large hyperpolarization-activated current (Ih) (>200 pA at -115 mV) and slow pacemaker-like firing rate (<5 Hz) (*25*).

Recording electrodes were pulled from borosilicate glass capillaries (1.5/0.86 mm OD/ID) with a micropipette puller (Sutter Instrument Co., model P-97). The resistance of patch electrodes was ~4.0 MΩ. Whole-cell patch-clamp experiments were performed with a Multiclamp 700A amplifier and Digidata 1322A data acquisition system (Molecular Devices). Whole-cell recordings were carried out at 30 ^oC with the internal solution containing (in mM): 125 K-gluconate, 5 KCl, 1 $MgCl_2$, 1 EGTA, 10 HEPES, 10 Glucose, 2 ATP, 0.5 GTP, and 10 phosphocreatine, pH 7.2-7.3, ~295 mOsm. The whole-cell patch-clamp configuration was first set up at in voltage-clamp mode (-70 mV), and the holding current was required to be smaller than 200 pA. Then, we changed to current-clamp mode for spontaneous action potential (sAP) recordings. Generally, a small current (<50 pA) needed to be injected for holding the membrane potential at -45 mV. After completing sAP recordings, it was changed to voltage-clamp mode for I_h-current

recordings for validation of DAergic identity. I_h-currents were induced by hyperpolarizing voltage steps (-40 to -130 mV, with 15 mV increments).

Behavioral Seeking

Following the last day of SA (cocaine, saline or food), animals were injected bilaterally intra-VTA with one of the following viral constructs: lenti-H3.3WT or lenti-H3.3Q5A (*vs.* empty lentiviral vector alone). Animals were left untouched in home cages for 30 days before behavioral testing. Following a 30 day withdrawal period, animals were reintroduced to the SA box and allowed to respond to the 'active' *vs.* 'inactive' lever for 1 hr. During this period, rats did not receive a reward, only the cue-light that was previously paired to the reward.

Fast-Scanning Cyclic Voltammetry (FSCV)

Animals were allowed to SA for cocaine (6 hr/day) for 10 days followed by bilateral injections intra-VTA with lenti-empty, lenti-H3.3WT or lenti-H3.3Q5A. After 30 days of WD, animals were placed back into SA boxes and allowed to respond for the 'active' lever and drug associated cue-light (no cocaine was administered) for 1 hr. Immediately following drug-seeking behavior, animals were euthanized and tissues were prepared for FSCV.

Ex vivo FSCV was used to characterize dopamine release in nucleus accumbens (NAc), as described in detail previously (*26*). Experimenters were blind to the testing conditions. A vibrating tissue slicer was used to prepare 300 μm-thick coronal brain sections containing NAc, which were immersed in oxygenated ACSF containing (in mM): NaCl (126), KCl (2.5), NaH_2PO_4 (1.2), $CaCl_2$ (2.4), $MgCl_2$ (1.2), $NaHCO_3$ (25),

glucose (11), L-ascorbic acid (0.4), with pH adjusted to 7.4. Slices were transferred to testing chambers containing ACSF at 32 °C with a 1 ml min^{-1} flow rate. A carbon fiber microelectrode (100–200 μM length, 7 μM radius) and bipolar stimulating electrode were placed into the NAc core region. Dopamine release was evoked by a single electrical pulse (300 μA, 4 ms, monophasic) applied to the tissue every 5 min. Extracellular dopamine levels were recorded by applying a triangular waveform (−0.4 to +1.2, to −0.4 V versus Ag/AgCl, 400 μV s^{-1}). Once the peak of evoked dopamine release was stabilized (three collections with <10% variability), the amount of evoked dopamine release and a maximal rate of uptake (V_{max}) were assessed. Subsequently, input output curves were conducted by varying the stimulation intensity – 100, 200, 300, 400, 500, 750, 900uA. The stimulation intensity that evoked the maximum level of dopamine release was recorded. For subsequent experiments, the minimum stimulation intensity that was capable of evoking the maximum possible dopamine release was used within each animal. Tonic and phasic stimulations were applied to slices, to determine the responsivity of terminals in NAc to tonic and phasic firing parameters. Tonic stimulations consisted of one pulse stimulations. Phasic stimulations consisted of five pulses at either 5, 10 or 20 Hertz. These stimulation parameters were selected based on the physiological firing properties of VTA dopamine neurons *in vivo*.

Recording electrodes were calibrated by recording responses (in electrical current; nA) to a known concentration of dopamine (3 μM) using a flow-injection system. This was used to convert an electrical current to a dopamine concentration.

Voltammetric data analysis

Demon voltammetry and analysis software was used for all analysis of FSCV data (*27*). Data were modeled using both peak and decay and Michaelis–Menten kinetics to determine dopamine release. For statistical comparisons of FSCV experiments, we first ran non-linear regression, EC50 analyses with the null hypothesis being that the EC50 ratios would be the same for all data sets tested. This null hypothesis was rejected, favoring the alternative hypothesis that the EC50 ratios are different ($p=0.0007$). Given that the curves were deemed to statistically different from one another, we performed a two-way ANOVA, repeated measures analysis on these data, indicating significant main effects of stimulation intensity and subject (**$p<0.01$), and significant Bonferroni *post hoc* comparisons of group means comparing H3.3Q5A *vs.* H3.3 WT (*$p<0.05$).

Note that we have shown previously that surgery, saline exposure and cues do not affect these measures using the exact same voltammetric procedure (*28, 29*).

Cocaine Sensitization

Rats were bilaterally injected intra-VTA with either lenti-H3.3WT or lenti-H3.3Q5A and given 21 days to allow for maximal viral expression. Prior to testing, rats were habituated to both i.p. injections and locomotor boxes. For habituation, rats were given two days of saline i.p. injections (only second day locomotor responses were recorded), and then individually placed into locomotor boxes–plexiglass chambers, which contained infrared beams to detect movement–for 30 min. Following 2 days of habituation, animals were given cocaine injections i.p. (10 mg/kg) for 5 days, and then tested every other day (i.e.

days 1, 3, 5) in the locomotor boxes for 30 min per session. All testing was conducted in a dark room during the light phase of the animals' light/dark cycle.

Statistical Analysis

For all behavioral testing and molecular experiments involving more than two treatments and time points, two-way or one-way ANOVAs were performed with subsequent Bonferroni or Tukey's *post hoc* analyses, and/or *a posteriori* t-tests. In molecular analyses, all animals used were included as separate *n*s (i.e., samples were not pooled). All of the data presented as being statistically significant were examined for normality against a Gaussian distribution, using both Shapiro-Wilk and Kolmogorov-Smirnov tests, indicating that all of our data pass normality (alpha=0.05). Significance was determined at $p<0.05$. All data are represented as mean ± SEM. See FSCV Methods for further details of statistical comparisons.

Main Text Figure Legends (Full with Statistics)

Fig. 1: Histone H3 dopaminylation in VTA is dysregulated by cocaine

(**A**) Western blot analysis of H3Q5dop in human postmortem VTA tissues from cocaine dependent subjects *vs.* matched controls (*n*=8-11/group, Student's *t* test was used, *$p\leq0.05$). Total H3 was used as a normalization control. No changes were observed in H3K4me3Q5dop, H3K4me3, H3, or Tgm2 expression ($p>0.05$; see fig. S5 for quantifications). (**B**) Experimental timeline of cocaine SA (extended access), followed by tissue collection time points during WD. (**C**) Number of infusions earned in daily 6 hr (extended access, FR5) test sessions in rats self-administering 0.5 mg/kg/infusion cocaine

or saline (*n*=7-10/group) for 10 days [extended access, cocaine *vs.* saline: two-way repeated measures ANOVA, with Bonferroni *post hoc* analysis *vs.* day 1, **p≤0.01, **** p≤0.0001). (**D**) Western blot analysis of H3Q5dop in VTA tissues (0 *vs.* 1 *vs.* 30 d WD) from extended access cocaine *vs.* saline SA rats (data shown as a normalized saline:cocaine ratio with saline set to 1, as depicted by the dotted line; *n*=7-11/group, two-way ANOVA with Bonferroni *post hoc* analysis, **p≤0.01, ***p≤0.001, or an *a posteriori* Student's *t* test, $^{\#\#}$p≤0.01, cocaine *vs.* saline at 0 d). No changes were observed in H3K4me3Q5dop, H3K4me3, H3, or Tgm2 expression (p>0.05; see fig. S5 for quantifications). Data presented as average ± SEM.

Fig. 2: H3Q5dop in VTA contributes to cocaine-mediated gene expression

(**A**) Immunofluorescence images of rat VTA transduced with a lentiviral vector expressing H3.3Q5A-HA-EF1-RFP overlayed with a nuclear co-stain (DAPI) at either 20x or 100x objective. (**B**) Western blot analysis of H3Q5dop in rat VTA tissues infected with lentiviral vectors expressing either empty vector or H3.3 WT *vs.* H3.3Q5A viruses (*n*=4-8/group; one-way ANOVA with Tukey's *post hoc* analysis, *p≤0.05 or an *a posteriori* Student's *t* test, $^{\#}$p≤0.05). H3K4me3Q5dop was not affected by transduction with H3.3Q5A (p>0.05). Total H3 was used as a normalization control. (**C**) Experimental timeline of SA (extended access cocaine *vs.* saline) RNA-seq experiment following viral transduction with either empty vector or H3.3 WT *vs.* H3.3Q5A viruses (*n*=7-8/group). (**D**) Key for RRHO maps describing the extent and directionality of overlap between differential gene expression lists in Fig. 2 E. (**E**) RRHO maps comparing differential expression between cocaine regulated gene lists–empty cocaine *vs.* saline and H3.3 WT

cocaine *vs.* saline (left), empty cocaine *vs.* saline and H3.3 Q5A cocaine *vs.* empty cocaine (middle), and H3.3 WT cocaine *vs.* saline and H3.3 Q5A cocaine *vs.* H3.3 WT cocaine (right). Each pixel represents the overlap between differential transcriptomes of the two conditions represented with the significance of overlap (-log10(corrected P-value) of a hypergeometric test color-coded. Overlap of differentially expressed protein coding genes (DEx PCGs) ($p<0.05$ via pairwise assessments) in VTA tissues comparing (**F**) cocaine *vs.* saline (empty) or (**G**) cocaine *vs.* saline (H3.3 WT) to H3.3Q5A *vs.* empty or H3.3 WT (cocaine) animals, respectively. Heat maps of overlapping genes obtained from RNA-seq data comparing (**H**) cocaine *vs.* saline (empty) and H3.3Q5A *vs.* empty (cocaine) animals or (**I**) cocaine *vs.* saline (H3.3 WT) and H3.3Q5A *vs.* H3.3 WT (cocaine) animals (720 and 211 PCGs, respectively) using normalized RNA expression values (averaged between replicates) to generate z-scores for each row. Note that ~95%-87% of all overlapping genes display significant reversals in gene expression by H3.3Q5A, respectively. (**J**) Kegg 2019 pathway enrichment analysis for the 211 overlapping PCGs displaying reversals in cocaine mediated gene expression from Fig. 2, G and I above (adjusted $p<0.05$). Data presented as average ± SEM.

Fig. 3: Attenuating H3Q5dop expression in VTA following extended access cocaine reduces drug-seeking associated DA release into ventral striatum

(**A**) Electrophysiological assessments of spontaneous action potential (sAP) frequency in VTA DAergic neurons from cocaine naïve rats infected with either empty vector, H3.3 WT or H3.3Q5A (*n*=9-15 cells from 3-4 rats per virus) viruses (one-way ANOVA with Tukey's *post hoc* analysis, *$p\leq0.05$, **$p\leq0.01$). Representative sAP traces are provided.

(**B**) Experimental timeline of cocaine SA (extended access) FSCV experiments following viral transduction with either H3.3 WT or H3.3Q5A and 1 hr of cocaine-seeking. Current *vs.* time (**C**) traces and (**D**) color plots demonstrating reduced DA release (evoked) in NAc of H3.3Q5A *vs.* empty/H3.3 WT (VTA) expressing animals. These data are quantified as (**E**) input/output curves (current *vs.* stimulation intensity) [*n*=3/group, two-way repeated measures ANOVA, significant main effects of stimulus intensity ($p=0.0016$) and subject ($p=0.0018$), with Bonferroni *post hoc* analysis comparing group means, *$p\leq0.05$; H3.3 Q5A *vs.* H3.3 WT]. This analysis followed non-linear regression, EC50 analyses with the null hypothesis being that the EC50 ratios would be the same for all data sets tested. This null hypothesis was rejected, favoring the alternative hypothesis that the EC50 ratios are different ($p=0.0007$). (**F**) Baseline DA release into NAc was similarly found to be reduced by H3.3Q5A (*n*=3/group, one-way ANOVA–$p\leq0.05$–with an *a posteriori* Student's *t* test, $^{\#}p\leq0.05$). Data presented as average ± SEM.

Fig. 4: Reducing H3Q5dop in VTA attenuates cocaine-seeking

(**A**) Experimental timeline of cocaine SA (extended access) drug-seeking experiments following viral transduction with either empty vector, H3.3 WT or H3.3Q5A viruses. (**B**) After 10 days of extended access cocaine [with escalation of intake observed, *n*=7-8/group, empty vector and H3.3 WT *vs.* H3.3Q5A (cocaine): two-way repeated measures ANOVA, with Bonferroni *post hoc* analysis *vs.* day 1, *$p\leq0.05$ – **** $p\leq0.0001$], rats were infected intra-VTA with one of the three viral vectors (on day 11), followed by 30 d of WD and (**E**) 1 hr of cocaine seeking; the total number of active responses is reduced in

H3.3Q5A rats *vs.* H3.3 WT controls (one-way ANOVA with Tukey's *post hoc* analysis, *$p \leq 0.05$ or an *a posteriori* Student's *t* test, $^{\#}p \leq 0.05$). Data presented as average ± SEM.

Supplemental Figures and Legends

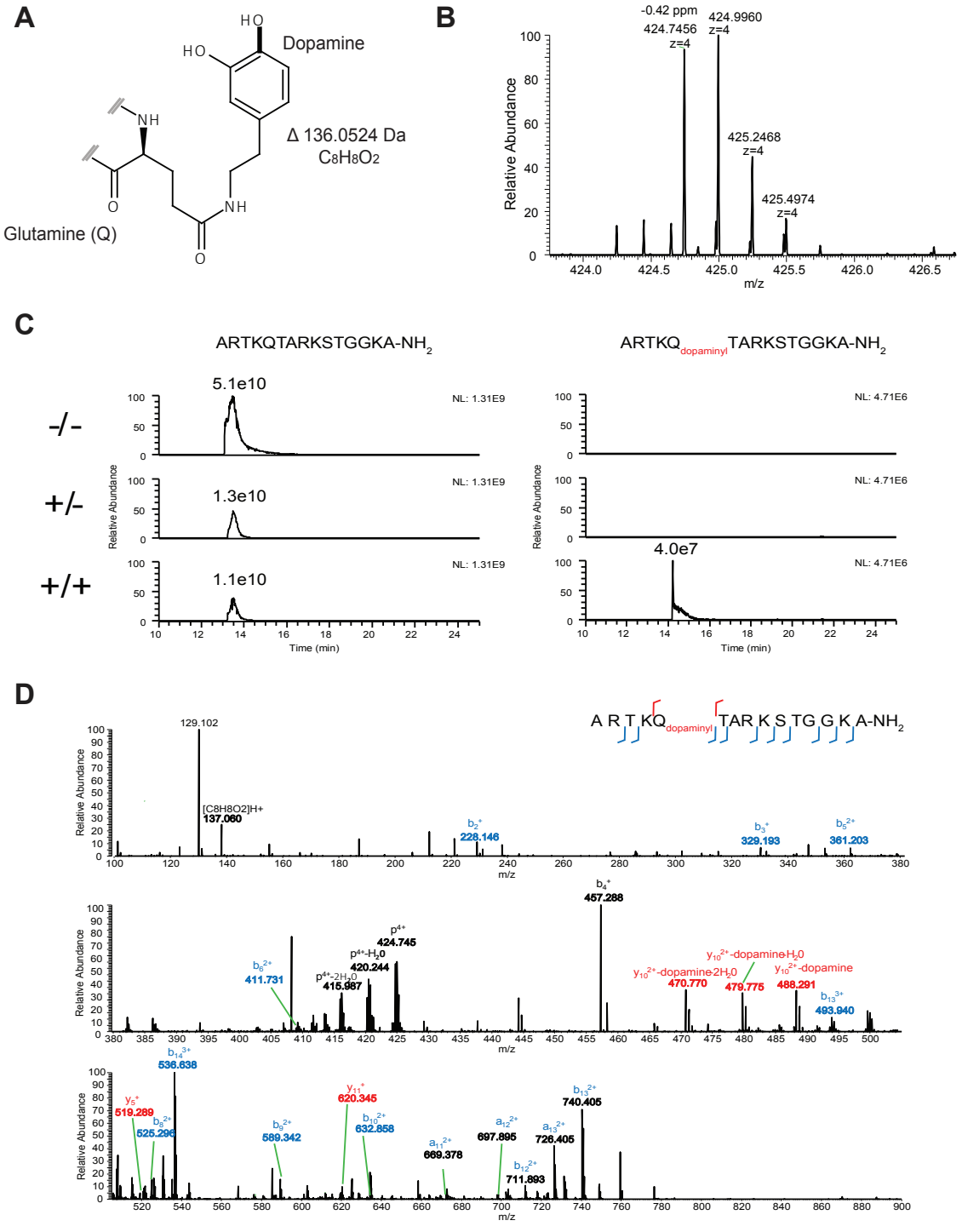

fig. S1: Histone H3Q5 is a substrate for dopaminylation *in vitro*

(**A**) Proposed structure of dopaminylated glutamine. (**B**) High resolution/high mass accuracy mass spectrum of the quadruply charged dopaminylated H3 tail peptide (ARTKQTARKSTGGKA-NH_3; +DA/+TGM2 condition). The difference between measured and expected mass of the amidated peptide was 0.42 ppm. (**C**) Ion traces of the amidated H3 tail peptide with (right panels) and without (left panels) dopaminylated glutamine. Top, middle and bottom panels show signals measured under –/–, –/+ and +/+ (DA/TGM2) conditions, respectively. Precursor masses were extracted using a 5 ppm window. (**D**) Tandem MS of the glutamine 5 dopaminylated H3 tail peptide (+DA/+TGM2 condition). Selected fragment ions (y and b) are labeled. Top panel displays the mass to charge (m/z) region from m/z 100-380, while the middle and bottom panels shows m/z 380-510 and m/z 510 to 900, respectively. Vertical lines in red and blue within the peptide sequence are used to highlight simplified peptide fragmentation.

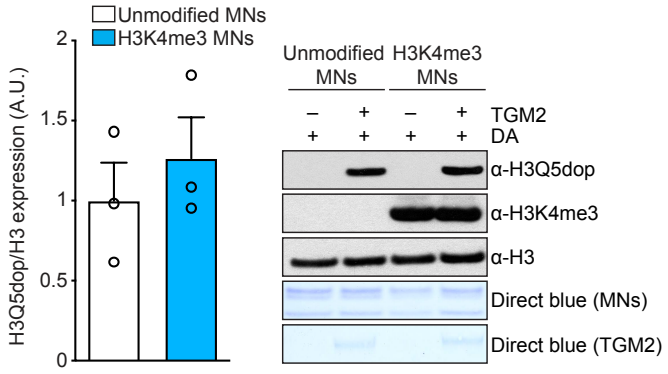

fig. S2: TGM2 dopaminylates H3Q5 equally in the absence or presence of adjacent K4me3

TGM2 dopaminylation assays on unmodified *vs.* H3K4me3 mononucleosomes (*n*=3/nucleosome type, two-tailed Student's t-test; p>0.05). Total H3 and direct blue staining are provided as a loading controls. H3K4me3 mononucleosomes were validated by blotting for the mark. Data presented as average ± SEM.

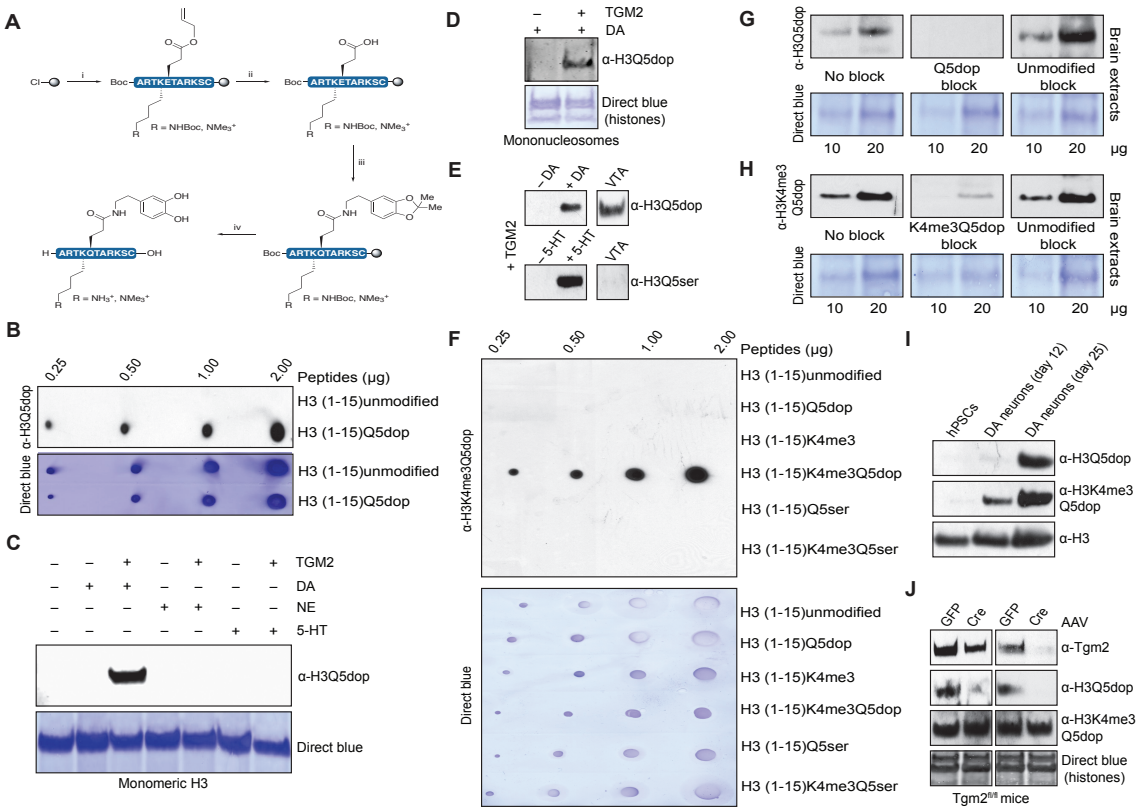

fig. S3: H3Q5dop and H3K4me3Q5dop antibody validations

(**A**) Synthesis of dopaminylated H3 peptides. Peptide backbones were (i) synthesized on 2-Cl trityl resin using standard Fmoc-strategy solid-phase synthesis (canonical side-chain protecting groups are omitted for clarity). Allyl-protected glutamate and either N_ε-Boc or N_ε-Me_3 lysine were incorporated at positions 5 and 4, respectively. Fully assembled peptides were then (ii) allyl deprotected, (iii) functionalized with dopamine acetonide and finally (iv) cleaved from the resin with concomitant side-chain deprotection. (**B**) Peptide dot blot titrations testing the α-H3Q5dop antibody's reactivity against unmodified *vs.* Q5dop peptides. Direct blue staining was used to control for peptide loading. (**C**) WB analysis of TGM2-based monoaminylation assays on unmodified monomeric H3 demonstrating that the α-H3Q5dop antibody only detects signal when H3 has been transamidated with DA (*vs.* 5-HT and norepinephrine/NE). Direct blue staining was used

to control for protein loading. (**D**) Western blotting analysis of TGM2 dopaminylation assays on unmodified mononucleosomes revealing that the α-H3Q5dop antibody detects signal only when the nucleosomes have been transamidated with DA. DB staining was used to control for protein loading. (**E**) H3Q5dop *vs.* H3Q5ser western blotting analysis indicating that while both antibodies detect their appropriate modifications in enzymatic TGM2 assays using donor dopamine *vs.* serotonin, respectively, only appreciable signal for H3Q5dop is observed in VTA lysates (**F**) Peptide dot blot titrations testing the α-H3K4me3Q5dop antibody's reactivity against various peptides; note that linear signal was only observed with the K4me3Q5dop peptide. Direct blue staining was used to control for peptide loading. Peptide competition (i.e., no block *vs.* unmodified H3 block *vs.* dopaminyl blocks/single or dual) western blotting analysis of lysates from rat brain indicating the specificity of our (**G**) α-H3Q5dop and (**H**) α-H3K4me3Q5dop antibodies *in vivo*. (**I**) Western blotting analysis of H3Q5dop and H3K4me3Q5dop (*vs.* total H3) in human pluripotent stem cells (hPSCs) and hPSC derived dopaminergic neurons at days 12 and 25 of differentiation [provided by Dr. Kristen Brennand (ISMMS), and generated using established protocols (*30*)]. These data demonstrate that while the dopaminyl marks are absent pre-differentiation (when dopamine is not present), both are greatly enhanced in their expression as dopaminergic neuronal identity is achieved. (**J**) Viral mediated knockdown (AAV-Cre *vs.* AAV-GFP) of Tgm2 of adult $Tgm2^{fl/fl}$ mice results in reduced expression of H3Q5dop, but not H3K4me3Q5dop, in VTA. Direct blue was used as a loading control.

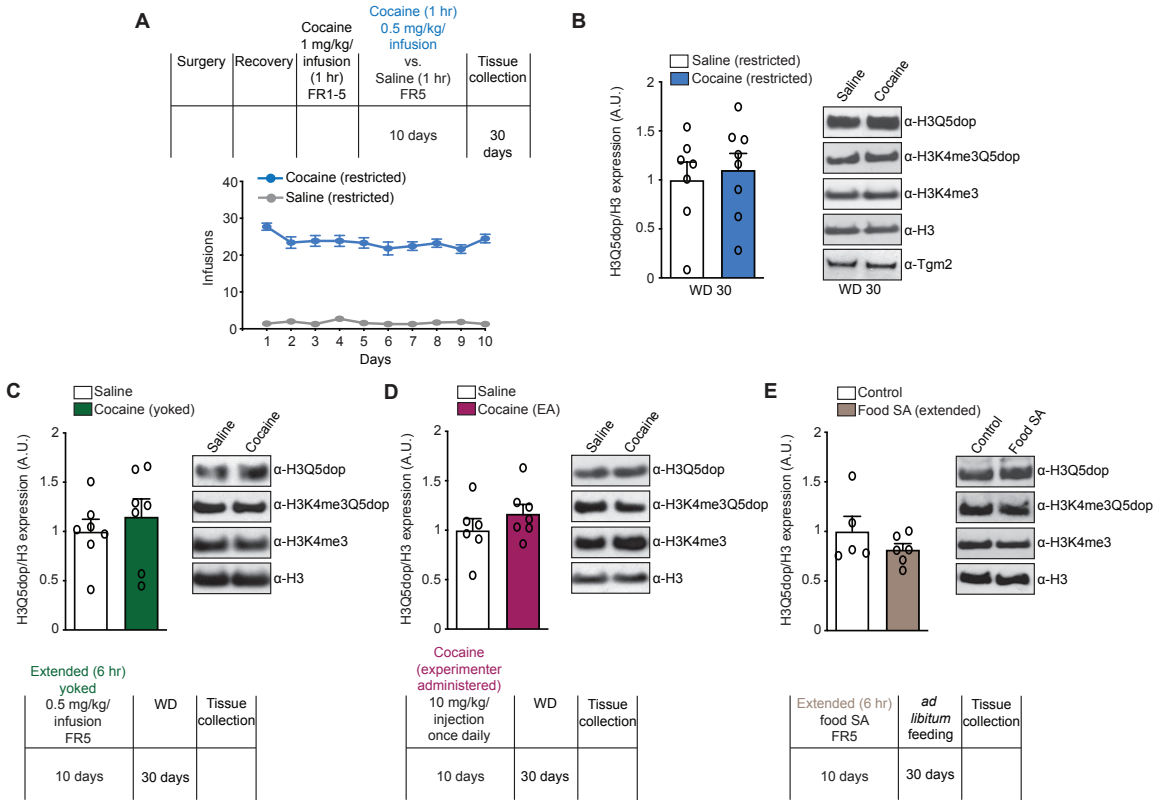

fig. S4: H3Q5dop remains unaffected by restricted access cocaine, and its accumulation in VTA requires volitional administration of a drug reward

(**A**, top) Experimental timeline of cocaine SA (restricted), followed by tissue collection time points during WD. (**A**, bottom) Number of infusions earned in daily 1 hr (restricted access, FR5) test sessions in rats self-administering 0.5 mg/kg/infusion cocaine or saline (*n*=7-22/group) for 10 days (**B**) Western blot analysis of H3Q5dop in VTA tissues (30 d WD) from restricted access cocaine *vs.* saline SA rats (*n*=7-8/group, p>0.05). No changes were also observed in H3K4me3Q5dop, H3K4me3, H3, or Tgm2 expression (p>0.05; see fig S5, F for quantifications). (**C**) Western blot analysis of H3Q5dop in VTA tissues (30 d WD) from yoked extended access cocaine *vs.* saline SA rats (*n*=7/group, p>0.05). No changes were observed in H3K4me3Q5dop, H3K4me3 or H3 expression (p>0.05; see fig

S5, G for quantifications). Experimental timeline is provided below. (**D**) Western blot analysis of H3Q5dop in VTA tissues (30 d WD) from experimenter-administered (EA) cocaine *vs.* saline rats (*n*=6-7/group, p>0.05). No changes were observed in H3K4me3Q5dop, H3K4me3 or H3 expression (p>0.05; see fig S5, H for quantifications). Experimental timeline is provided below. (**E**) Western blot analysis of H3Q5dop in VTA tissues (30 d *ad libitum*) from extended access food (natural reinforcer) *vs.* non-reinforcement control rats (*n*=5-6/group, p>0.05). No changes were observed in H3K4me3Q5dop, H3K4me3 or H3 expression (p>0.05; see fig S5, I for quantifications). Experimental timeline is provided below. Data presented as average ± SEM.

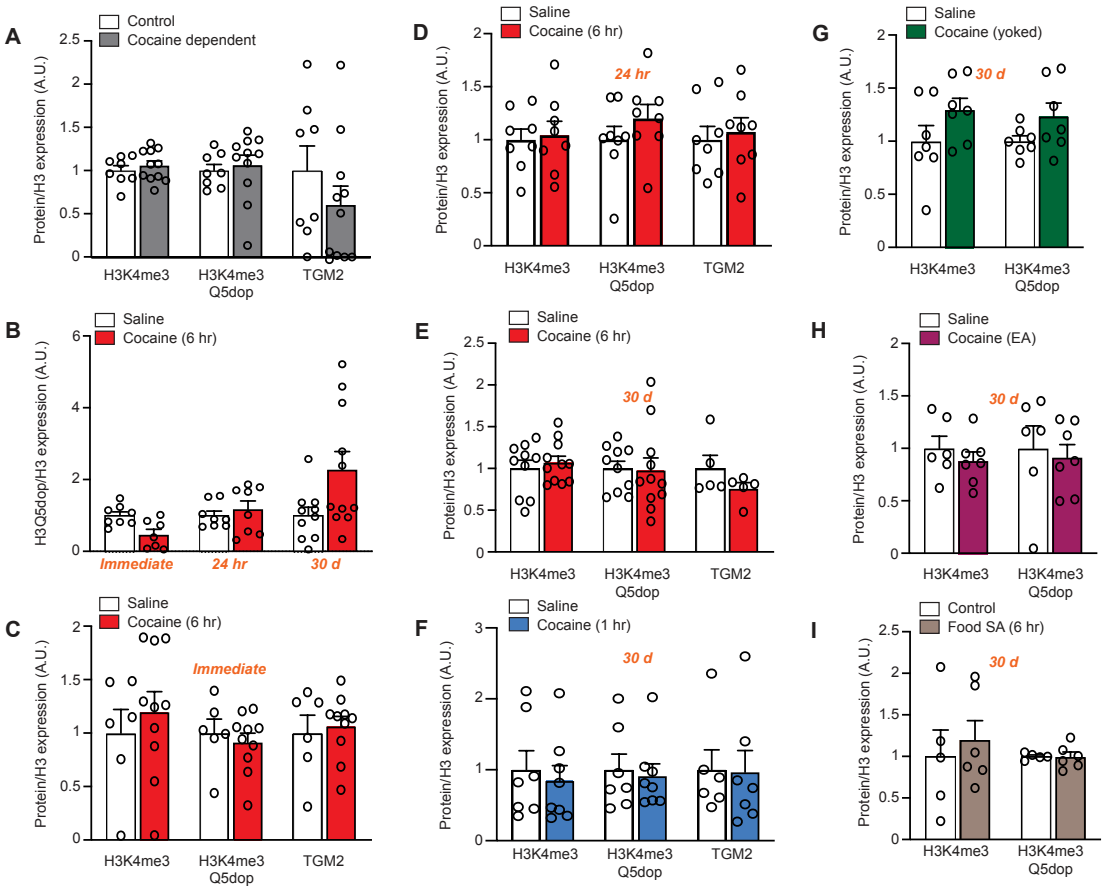

fig. S5: Quantifications of negative western blotting data in VTA

Related to (**A**) Fig. 1A, (**B-E**) Fig. 1D, (**F**) fig. S4B, (**G**) fig. S4D, (**H**) fig. S4E and (**I**) fig. S4F. Data presented as average ± SEM (all p>0.05 with the exception of saline *vs.* extended access cocaine H3Q5dop/H3 data from Fig. 1, D).

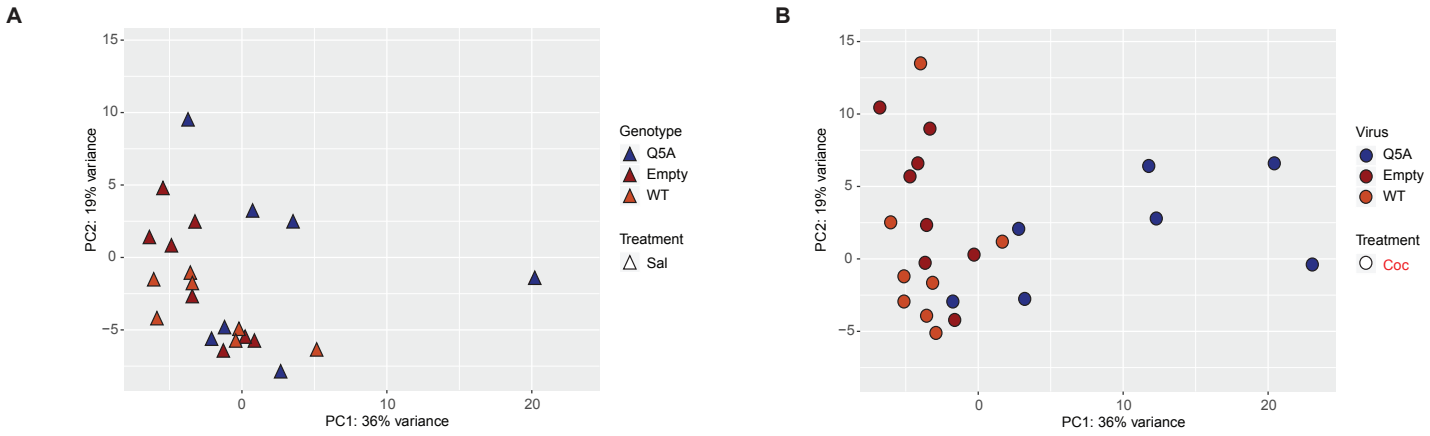

fig. S6: Principal component analysis (PCA) of samples used in RNA-seq assessments

Related to Fig. 2. Analysis of RNA-seq sample variance across VTA virally infected tissues (empty, H3.3 WT and H3.3 Q5A) from (**A**) saline or (**B**) extended access cocaine self-administering rats. While all viral groups generally cluster together in saline treated animals, the H3.3 Q5A viral group displays clear divergence from the empty vector and H3.3 WT control groups following cocaine, as is reflected in the differential analyses depicted in Fig. 2.

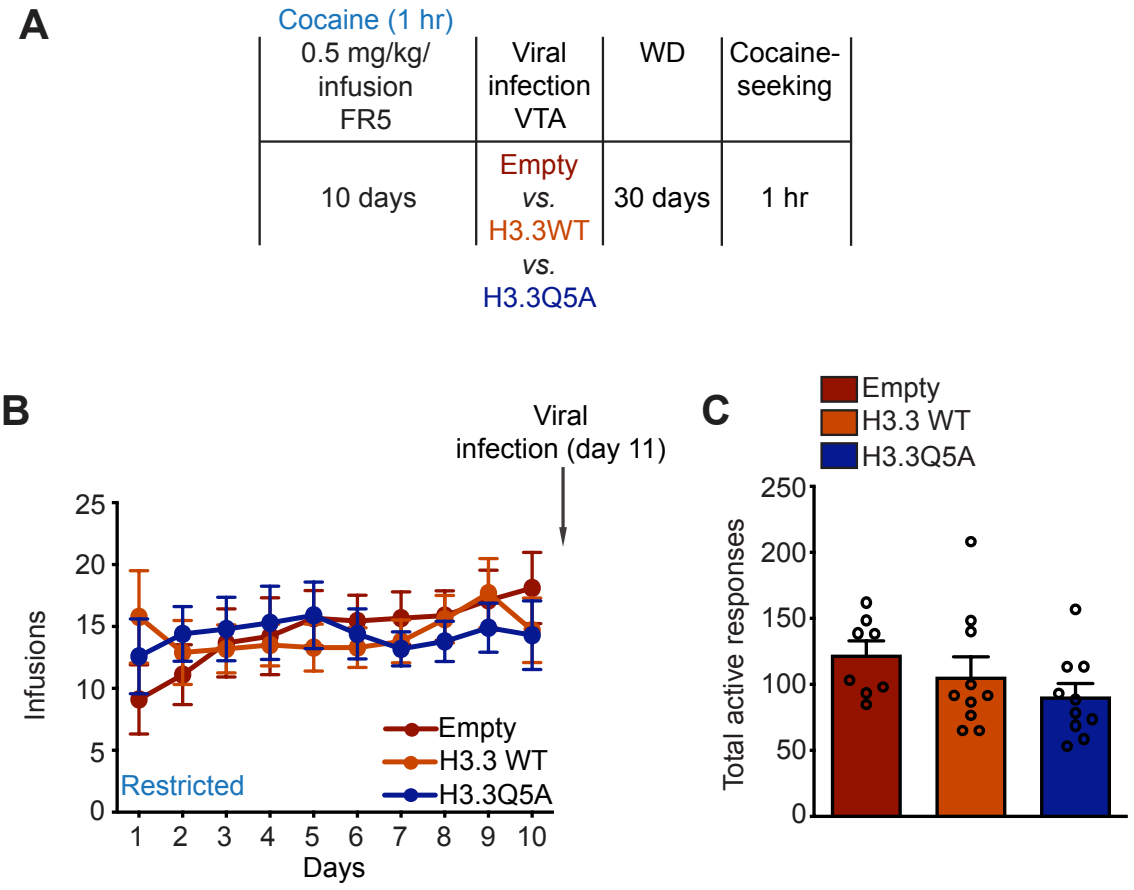

fig. S7: Reducing H3Q5dop in VTA has no effect on cocaine-seeking following restricted access to cocaine

(**A**) Experimental timeline of cocaine SA (restricted access) drug-seeking experiments following viral transduction with empty vector or H3.3 WT controls *vs.* H3.3Q5A. (**B**) Following 10 days of restricted access cocaine (*n*=9-10/group, two-way ANOVA was

used, $p>0.05$), rats were infected intra-VTA with one of the three viruses (day 11), followed by 30 d of WD and (**C**) 1 hr of cocaine seeking; the total number of active responses recorded between viral conditions was unaffected (n=8-10/group, one-way ANOVA was used, $p>0.05$). Data presented as average ± SEM.

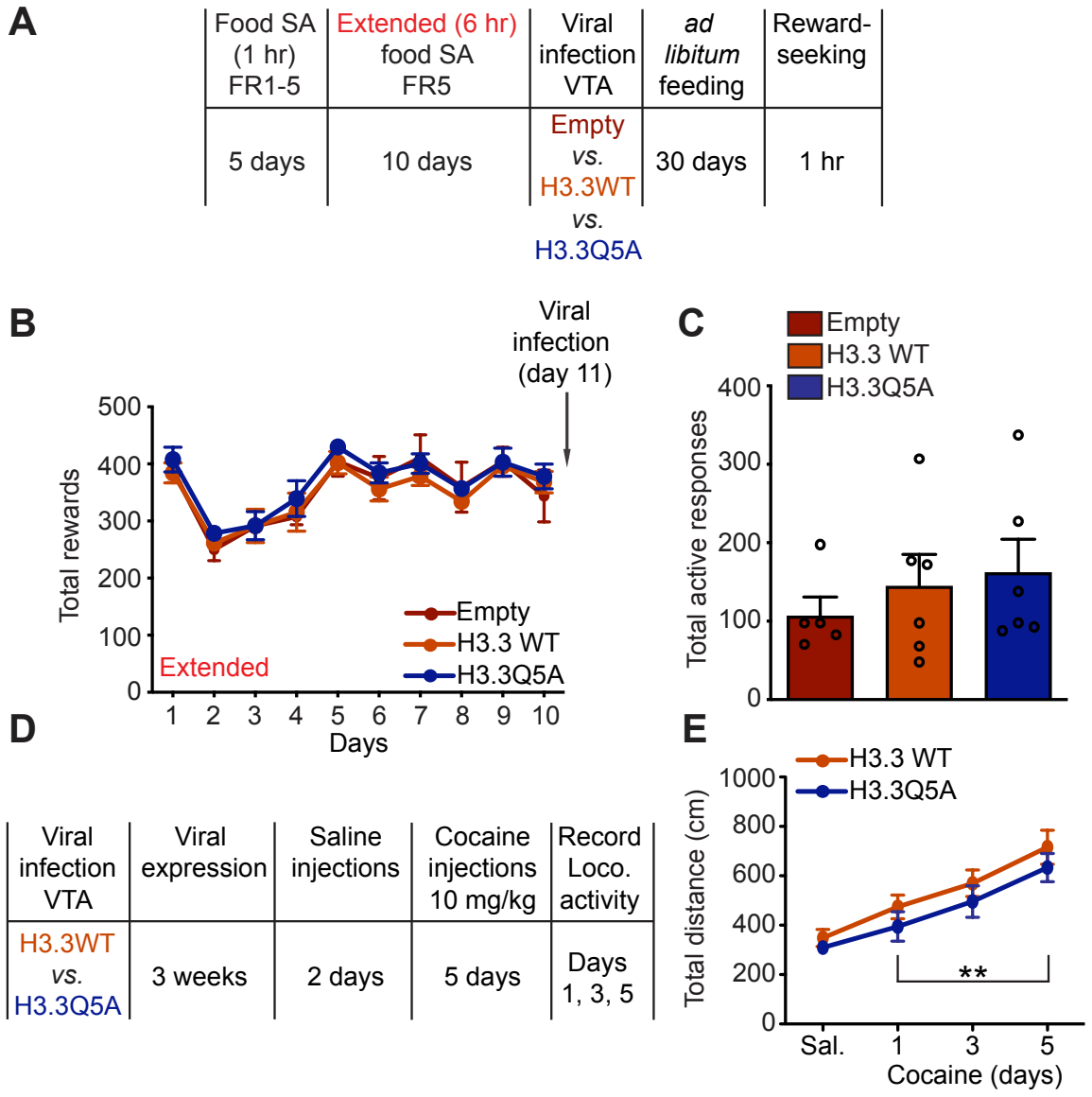

fig. S8: Blocking H3Q5dop in VTA affects neither seeking for a natural reward nor cocaine-induced psychomotor sensitization

(**A**) Experimental timeline of food SA (extended access) seeking experiments following viral transduction with empty vector or H3.3 WT controls *vs.* H3.3Q5A. (**B**) Following 10 days of extended access food SA (*n*=5-6/group, two-way ANOVA was used, p>0.05),

rats were infected intra-VTA with empty vector, H3.3 WT or H3.3Q5A (day 11), followed by 30 d of *ad libitum* feeding and (**C**) 1 hr of reward-seeking; the total number of active responses recorded between viral conditions was unaffected (n=5-6/group, one-way ANOVA was used, $p>0.05$). (**D**) Experimental timeline of cocaine sensitization (extended access) experiment following viral transduction with either H3.3 WT or H3.3Q5A. (**E**) Psychomotor sensitization was measured over the course of five days (following one day of habituation/single saline injection) after cocaine injections (1/day, i.p.); while all rats displayed increased locomotor activity with repeated injections (n=7/group, Student's t test was used comparing cocaine days 1 *vs.* 3, ** $p\leq0.01$), no differences between viruses were observed (Student's t test was used comparing H3.3 WT *vs.* H3.3Q5A on days 1, 3 and 5 – $p>0.05$). Data presented as average ± SEM.

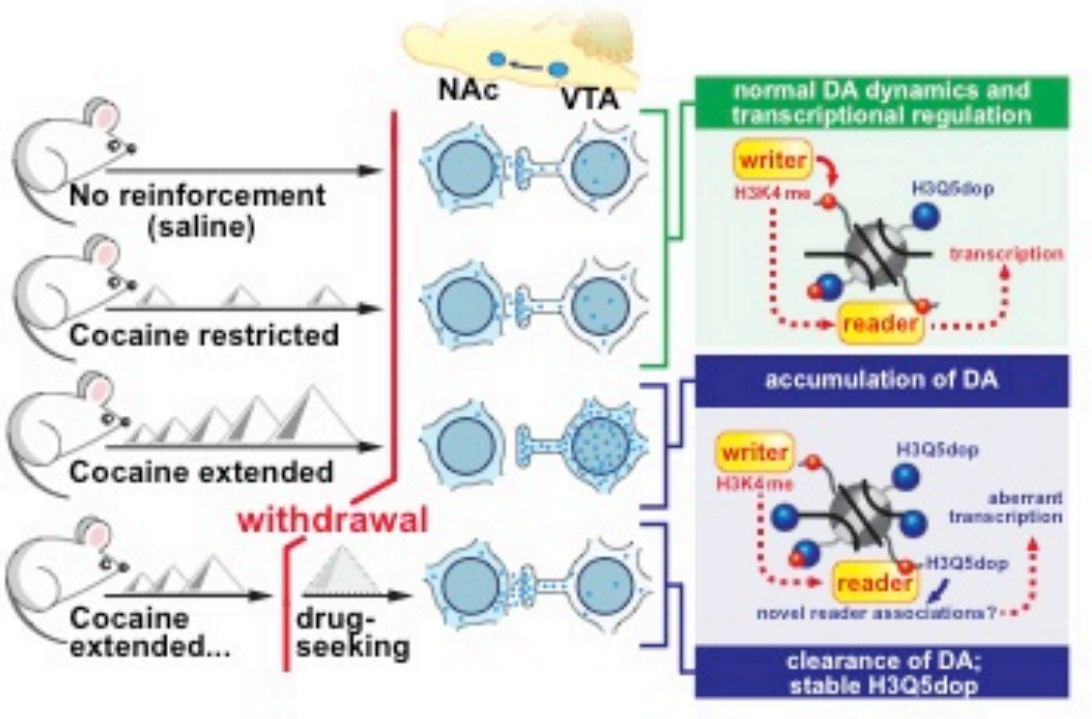

fig. S9: Working model

Our data indicate that H3Q5dop accumulates in VTA following prolonged WD from extended, but not restricted, access cocaine (*vs.* their respective saline controls) leading to cocaine mediated gene expression, enhanced drug-seeking-induced DA release into NAc and increased vulnerability to relapse associated behaviors. While cocaine-seeking or drug re-exposures likely lead to clearance of pathophysiological levels of DA in VTA cell bodies/nuclei, we hypothesize that aberrant H3Q5dop may be stable, thereby contributing to the persistence of the addicted state.

Supplementary Sequencing Data Tables

Excel file including Supplementary Data Tables 1-5, which contain processed RNA-seq data from virally infected brain and associated pathway enrichment analysis.

References and Notes

1. L. A. Farrelly, R. E. Thompson, S. Zhao, A. E. Lepack, Y. Lyu, N. V. Bhanu, B. Zhang, Y. E. Loh, A. Ramakrishnan, K. C. Vadodaria, K. J. Heard, G. Erikson, T. Nakadai, R. M. Bastle, B. J. Lukasak, H. Zebroski 3rd, N. Alenina, M. Bader, O. Berton, R. G. Roeder, H. Molina, F. H. Gage, L. Shen, B. A. Garcia, H. Li, T. W. Muir, I. Maze, Histone serotonylation is a permissive modification that enhances TFIID binding to H3K4me3. *Nature* **567**, 535–539 (2019). doi:10.1038/s41586-019-1024-7 Medline

2. D. J. Walther, J.-U. Peter, S. Winter, M. Höltje, N. Paulmann, M. Grohmann, J. Vowinckel, V. Alamo-Bethencourt, C. S. Wilhelm, G. Ahnert-Hilger, M. Bader, Serotonylation of small GTPases is a signal transduction pathway that triggers platelet alpha-granule release. *Cell* **115**, 851–862 (2003). doi:10.1016/S0092-8674(03)01014-6 Medline

3. J. W. Grimm, B. T. Hope, R. A. Wise, Y. Shaham, Incubation of cocaine craving after withdrawal. *Nature* **412**, 141–142 (2001). doi:10.1038/35084134 Medline

4. K. L. Conrad, K. Y. Tseng, J. L. Uejima, J. M. Reimers, L.-J. Heng, Y. Shaham, M. Marinelli, M. E. Wolf, Formation of accumbens GluR2-lacking AMPA receptors mediates incubation of cocaine craving. *Nature* **454**, 118–121 (2008). doi:10.1038/nature06995 Medline

5. C. L. Pickens, M. Airavaara, F. Theberge, S. Fanous, B. T. Hope, Y. Shaham, Neurobiology of the incubation of drug craving. *Trends Neurosci.* **34**, 411–420 (2011). doi:10.1016/j.tins.2011.06.001 Medline

6. J. W. Grimm, L. Lu, T. Hayashi, B. T. Hope, T.-P. Su, Y. Shaham, Time-dependent increases in brain-derived neurotrophic factor protein levels within the mesolimbic dopamine system after withdrawal from cocaine: Implications for incubation of cocaine craving. *J. Neurosci.* **23**, 742–747 (2003). doi:10.1523/JNEUROSCI.23-03-00742.2003 Medline

7. I. Maze, E. J. Nestler, The epigenetic landscape of addiction. *Ann. N. Y. Acad. Sci.* **1216**, 99–113 (2011). doi:10.1111/j.1749-6632.2010.05893.x Medline

8. H. D. Schmidt, J. F. McGinty, A. E. West, G. Sadri-Vakili, Epigenetics and psychostimulant addiction. *Cold Spring Harb. Perspect. Med.* **3**, a012047 (2013). doi:10.1101/cshperspect.a012047 Medline

9. R. Hummerich, J. O. Thumfart, P. Findeisen, D. Bartsch, P. Schloss, Transglutaminase-mediated transamidation of serotonin, dopamine and noradrenaline to fibronectin: Evidence for a general mechanism of monoaminylation. *FEBS Lett.* **586**, 3421–3428 (2012). doi:10.1016/j.febslet.2012.07.062 Medline

10. S. Cooper, A. J. Robison, M. S. Mazei-Robison, Reward Circuitry in Addiction. *Neurotherapeutics* **14**, 687–697 (2017). doi:10.1007/s13311-017-0525-z Medline

11. R. A. Wheeler, R. M. Carelli, Dissecting motivational circuitry to understand substance abuse. *Neuropharmacology* **56**, 149–159 (2009). doi:10.1016/j.neuropharm.2008.06.028 Medline

12. S. H. Ahmed, G. F. Koob, Transition from moderate to excessive drug intake: Change in hedonic set point. *Science* **282**, 298–300 (1998). doi:10.1126/science.282.5387.298 Medline

13. U. Shalev, J. W. Grimm, Y. Shaham, Neurobiology of relapse to heroin and cocaine seeking: A review. *Pharmacol. Rev.* **54**, 1–42 (2002). doi:10.1124/pr.54.1.1 Medline

14. H. M. Lesscher, L. J. Vanderschuren, Compulsive drug use and its neural substrates. *Rev. Neurosci.* **23**, 731–745 (2012). doi:10.1515/revneuro-2012-0066 Medline

15. V. Deroche-Gamonet, P. V. Piazza, Psychobiology of cocaine addiction: Contribution of a multi-symptomatic animal model of loss of control. *Neuropharmacology* **76**, 437–449 (2014). doi:10.1016/j.neuropharm.2013.07.014 Medline

16. R. Quirion, Y. Robitaille, J. Martial, J.-G. Chabot, P. Lemoine, C. Pilapil, M. Dalpé, Human brain receptor autoradiography using whole hemisphere sections: A general method that minimizes tissue artefacts. *Synapse* **1**, 446–454 (1987). doi:10.1002/syn.890010508 Medline

17. J. A. Hollander, H.-I. Im, A. L. Amelio, J. Kocerha, P. Bali, Q. Lu, D. Willoughby, C. Wahlestedt, M. D. Conkright, P. J. Kenny, Striatal microRNA controls cocaine intake through CREB signalling. *Nature* **466**, 197–202 (2010). doi:10.1038/nature09202 Medline

18. M. de Victoria Rodríguez, E. Brunet, M. Nocchetti, F. Presciutti, F. Costantino, Redox properties of LDH microcrystals coated with a catechol-bearing phosphonate derived from dopamine. *RSC Advances* **4**, 26912–26917 (2014). doi:10.1039/C4RA03660C

19. S. B. Plaisier, R. Taschereau, J. A. Wong, T. G. Graeber, Rank-rank hypergeometric overlap: Identification of statistically significant overlap between gene-expression signatures. *Nucleic Acids Res.* **38**, e169 (2010). doi:10.1093/nar/gkq636 Medline

20. E. Y. Chen, C. M. Tan, Y. Kou, Q. Duan, Z. Wang, G. V. Meirelles, N. R. Clark, A. Ma'ayan, Enrichr: Interactive and collaborative HTML5 gene list enrichment analysis tool. *BMC Bioinformatics* **14**, 128 (2013). doi:10.1186/1471-2105-14-128 Medline

21. M. V. Kuleshov, M. R. Jones, A. D. Rouillard, N. F. Fernandez, Q. Duan, Z. Wang, S. Koplev, S. L. Jenkins, K. M. Jagodnik, A. Lachmann, M. G. McDermott, C. D. Monteiro, G. W. Gundersen, A. Ma'ayan, Enrichr: A comprehensive gene set enrichment analysis web server 2016 update. *Nucleic Acids Res.* **44**, W90–W97 (2016). doi:10.1093/nar/gkw377 Medline

22. M. Kanehisa, S. Goto, KEGG: Kyoto encyclopedia of genes and genomes. *Nucleic Acids Res.* **28**, 27–30 (2000). doi:10.1093/nar/28.1.27 Medline

23. B. L. Warren, S. D. Iñiguez, L. F. Alcantara, K. N. Wright, E. M. Parise, S. K. Weakley, C. A. Bolaños-Guzmán, Juvenile administration of concomitant methylphenidate and fluoxetine alters behavioral reactivity to reward- and mood-related stimuli and disrupts ventral tegmental area gene expression in adulthood. *J. Neurosci.* **31**, 10347–10358 (2011). doi:10.1523/JNEUROSCI.1470-11.2011 Medline

24. S. W. Johnson, R. A. North, Two types of neurone in the rat ventral tegmental area and their synaptic inputs. *J. Physiol.* **450**, 455–468 (1992). doi:10.1113/jphysiol.1992.sp019136 Medline

25. D. Mao, K. Gallagher, D. S. McGehee, Nicotine potentiation of excitatory inputs to ventral tegmental area dopamine neurons. *J. Neurosci.* **31**, 6710–6720 (2011). doi:10.1523/JNEUROSCI.5671-10.2011 Medline

26. E. S. Calipari, B. Juarez, C. Morel, D. M. Walker, M. E. Cahill, E. Ribeiro, C. Roman-Ortiz, C. Ramakrishnan, K. Deisseroth, M.-H. Han, E. J. Nestler, Dopaminergic dynamics underlying sex-specific cocaine reward. *Nat. Commun.* **8**, 13877 (2017). doi:10.1038/ncomms13877 Medline

27. J. T. Yorgason, R. A. España, S. R. Jones, Demon voltammetry and analysis software: Analysis of cocaine-induced alterations in dopamine signaling using multiple kinetic measures. *J. Neurosci. Methods* **202**, 158–164 (2011). doi:10.1016/j.jneumeth.2011.03.001 Medline

28. E. S. Calipari, T. J. Beveridge, S. R. Jones, L. J. Porrino, Withdrawal from extended-access cocaine self-administration results in dysregulated functional activity and altered locomotor activity in rats. *Eur. J. Neurosci.* **38**, 3749–3757 (2013). doi:10.1111/ejn.12381 Medline

29. E. S. Calipari, M. J. Ferris, B. A. Zimmer, D. C. Roberts, S. R. Jones, Temporal pattern of cocaine intake determines tolerance vs sensitization of cocaine effects at the dopamine transporter. *Neuropsychopharmacology* **38**, 2385–2392 (2013). doi:10.1038/npp.2013.136 Medline

30. S. Kriks, L. Studer, Protocols for generating ES cell-derived dopamine neurons. *Adv. Exp. Med. Biol.* **651**, 101–111 (2009). doi:10.1007/978-1-4419-0322-8_10 Medline